Tricritical scaling and logarithmic corrections for the metamagnet $FeCl_2$

H.-T. Shang* and M. B. Salamon
Department of Physics and Materials Research Laboratory, University of Illinois at Urbana-Champaign, Urbana, Illinois 61801
(Received 10 March 1980)

The uniform (nonordering) magnetization and heat capacity of $FeCl_2$ have been measured simultaneously in the vicinity of the tricritical point. Using the peak in the heat capacity in the second-order region and the light scattering in the first-order region, we have determined the phase diagram for this metamagnetic tricritical point. A technique is described which permits simultaneous measurement of these properties using the ac calorimetric and Faraday rotation techniques. Data were collected along isotherms as functions of external field and were then corrected to internal field using the measured magnetization and demagnetizing factors. We demonstrate that the data for the magnetization and heat capacity do not satisfy scaling relations with classical exponents, $\phi=2$ and $\alpha_t=\frac{1}{2}$, but may be made to "collapse" in the predicted manner only when α_t is permitted to take an effective value $\alpha_t^{\rm eff}=0.65$. When logarithmic correction factors of the form $L(r)=1-a_6\ln(r)$ are included, however, the data collapse with *classical* exponents. The constant a_6 is a nonuniversal amplitude which we find to be $a_6=0.5\pm0.2$ and the field r is defined to vanish along the logarithmically corrected—and experimentally observed—second-order line. Along the first-order line, the behavior of the step change in magnetization is improved by logarithmic corrections, but the classical exponents are not fully recovered. The logarithmic factors occur in the scaled free energy such that, over any limited range of experimental data, they may be represented by power laws with effective exponents. The logarithmic factors appear to be more important for metamagnets such as $FeCl_2$ and $CsCoCl_3\cdot 2H_2O$ (which behaves similarly) than for ^{3}He-^{4}He mixtures.

I. INTRODUCTION

Although the possibility of an end point on a line of second-order transitions was explored first by Landau,[1] Griffiths[2] pointed out only recently that this should be considered the intersection of three critical lines, and is thus properly termed a tricritical point. The scaling analysis of this special point, developed by Riedel,[3] was generalized by Chang *et al.*[4] Riedel and Wegner[5] employed the renormalization method to obtain classical (mean-field) exponents and subsequently extended the treatment to include logarithmic corrections to mean-field behavior.[6] Using diagrammatic analysis, Stephen, Abrahams, and Straley[7] (SAS) examined the logarithmic corrections and obtained a free energy which differs significantly from that of Wegner and Riedel[6] (WR). A number of subsequent developments has substantiated the prediction that the tricritical point is characterized by classical critical exponents, with a cross over to critical behavior governed by an exponent $\phi=2$, but with fractional powers of logarithms as correction factors.

The experimental situation is far less clear. A detailed analysis[8] of the ^{3}He-^{4}He tricritical point has demonstrated the correctness of the scaling approach and yielded the expected classical exponents. Metamagnetic tricritical behavior, which has been reviewed recently by Stryjewski and Giordano,[9] presents a less clear picture. While the early work by Giordano and Wolf[10] on DAG, along with certain results for $FeCl_2$,[11] support the classical values for the tricritical exponents, other results show quite significant deviations. Neutron data for $FeCl_2$ (Ref. 12) and a rather complete study of $CsCoCl_3\cdot 2H_2O$ (Ref. 13) have exponents quite far from classical values. No test for logarithmic corrections has been attempted previously for any metamagnetic tricritical point; no such corrections could be detected in ^{3}He-^{4}He mixtures. However, the nature of logarithmic correction factors is such that they are expected to be always present, but with nonuniversal amplitude. Thus, unobservability in one system does not preclude their detection in another. To set the stage for this study, we have adapted Table I from Ref. 9, in which the critical exponents without logarithmic corrections are summarized.

In this paper, we report results of experiments on the metamagnet $FeCl_2$ in the vicinity of the tricritical point. Our data on the uniform (nonordering) magnetization and the heat capacity, measured simultaneously, are sufficiently precise to permit a careful test of the predictions of scaling theory, including logarithmic corrections. Our results for the metamagnetic phase boundaries differ in detail from previous opti-

TABLE I. Experimental and theoretical tricritical exponents (adapted from Ref. 9).

Material	Author	α_t	β_μ^+	β_μ^-	β_μ	ϕ	β_1	β_t	β_t^{eff}	$\bar{\alpha}$	$\beta_\mu-\phi(1-\alpha_t)$
$FeCl_2$	Birgeneau *et al.*	···	1	0.36	···	~2	0.19	···	0.36	···	···
	Ref. 12			±0.04			±0.02		±0.04	···	···
	Griffin *et al.*	···	1.03	1.13	1.11	~2	···	···	···	···	···
	Ref. 11		±0.05	±0.14	±0.11				···	···	···
	Dillon, Jr., *et al.*	···	1.00	1.00	1.00	···	···	···	···	···	···
	Ref. 11		±0.02	±0.07	±0.08				···		
	Present work	0.65	···	···	0.63	~2	···	···	···	−0.35	0.07
	(effective exponents)	±0.05			±0.05					±0.05	±0.15
$CsCoCl_3\cdot 2D_2O$	Bongaarts *et al.*	0.65	0.7	0.7	0.65	2	0.3	0.15	0.36	···	0.05
	Ref. 13	±0.05	±0.4	±0.4	±0.20	±0.2	±0.1	±0.02	±0.05		±0.32
$Dy_3Al_5O_{12}$ (DAG)	Giordano *et al.*	0.52 ± 0.05	1	1	0.98	1.95	···	···	···	···	···
	Ref. 10				±0.05	±0.11					
Theory	Riedel *et al.*	1/2	1	1	1	2	1/2	1/4	1/2	−1/2	0
	Ref. 5										

cal determinations[11] but are in agreement with neutron data.[12] As with $CsCoCl_3\cdot 2H_2O$,[13] $FeCl_2$ requires a nonclassical value for the tricritical exponent α_t, but a classical value of ϕ, if scaling predictions are to hold in the absence of logarithmic corrections. All other exponents take on nonclassical values such that scaling laws hold. Over limited ranges, classical exponents can be employed, but significant deviations occur. We have no explanation for the discrepancies among the various results in Table I, but note that specific-heat results were essential to the determination of the correct position of the critical line.

Inclusion of logarithmic corrections as predicted by SAS results in a recovery of classical exponents in the scaling of both the magnetization and the heat capacity. A single adjustable parameter, the nonuniversal amplitude of the logarithmic terms, is required, but this replaces the adjustable critical exponent α_t which now has its classical value $\frac{1}{2}$. This amplitude has a value within the range predicted by SAS, but is significantly *smaller* than recently suggested by Stephen.[14] Preliminary analysis of the magnetization data, with and without logarithmic correction terms, has appeared previously.[15] Our principal results here include: the observation of logarithmic corrections to scaling, the first scaling of the heat capacity near a tricritical point, and a demonstration that the nonclassical exponents are a result of ignoring logarithmic factors which are, in fact, present.

In Sec. II we describe the theoretical results for tricritical scaling of the magnetization, including logarithmic factors, and derive similar expressions for the heat capacity. Following a description of the experimental methods in Sec. III, we test the results of Sec. II against our data. The approach is to demonstrate the failure of classical scaling, the improvement of data collapsing with nonclassical exponents, and finally, the recovery of classical exponents when the logarithmic factors are added. The analysis is separated into an analysis of the critical line and then the more difficult problem of the first-order line. Details of the behavior of the specific heat along the first-order line which have been reported previously, will not be repeated here.[15]

II. SCALING AT THE TRICRITICAL POINT

A. Conventional scaling theory

The scaling approach to tricritical phenomena, developed by Riedel,[3] Griffiths,[16] and Chang, Hankey, and Stanley,[4] assumes that the singular part of the free energy is, asymptotically, a generalized homogeneous function of a set of scaling variables μ_1, μ_2, and H_S:

$$G(H_S,\mu_1,\mu_2)=l^{-(2-\alpha_t)\phi}G(l^{\phi\Delta_t}H_S,l^{\phi}\mu_1,l\mu_2)\ , \quad (2.1)$$

where $\Delta_t=\beta_t\delta_t$. The quantities μ_1 and μ_2 are scaling fields which are functions of $H-H_t$ and $T-T_t$, where the tricritical point is at (T_t,H_t). The $\vec{\mu}_2$ axis (see Fig. 1) is asymptotically parallel to the critical line at the tricritical point, while $\vec{\mu}_1$ points away from the critical line (but not necessarily normal to $\vec{\mu}_2$). A necessary condition on μ_1 is that the critical line L_1 in the $H_s=0$ plane, be representable as

$$\mu_1^{\zeta}=K\mu_2^{\phi}\ , \quad (2.2)$$

where ϕ is the crossover exponent. The tricritical ex-

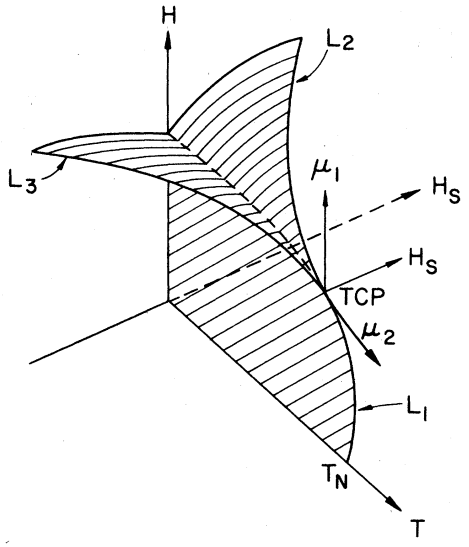

FIG. 1. Tricritical phase diagram showing the definition of the conventional scaling fields.

ponents can be subdivided into two classes: (i) those that describe the tricritical behavior by regarding the tricritical point as a special point on the line of critical points: α_t, β_t, γ_t, δ_t, $\bar{\alpha}$ and (ii) those that describe the tricritical behavior by regarding the tricritical point as an "ordinary" critical point: α_μ, β_μ, γ_μ, δ_μ, β_1. Sets (i) and (ii) are related through the crossover exponent ϕ. The exponents are predicted to have classical values, as listed in Table I.

Tricritical scaling theory[3] predicts that the singular part of any thermodynamic quantity $B(\mu_1, \mu_2)$ with critical exponent a, tricritical exponent a_t, and crossover exponent ϕ will satisfy

$$\mu_2^{-a_t\phi} B(\mu_1, \mu_2) = B^*(\mu_1/\mu_2^\phi) \ . \tag{2.3}$$

The scaling fields μ_1 and μ_2 are, in this case, analytic functions of H and T. The scaling function B^* depends only on the scale invariant quantity $Y_2 = \mu_1/\mu_2^\phi$ and may be singular along the critical line $Y_2 = K$ [cf. Eq. (2.2)]. In order to make a precise scaling hypothesis about the critical line it is necessary[4] to define a new variable

$$Y_2' = Y_2 - K \ . \tag{2.4}$$

The scaling function B^* now is expected to exhibit the following asymptotic behavior:

$$B^* \sim \begin{cases} Y_2'^{-a}, & \text{critical region } (Y_2' << 1) \\ Y_2^{-a_t}, & \text{tricritical region } (Y_2 >> 1) \end{cases} . \tag{2.5}$$

The use of Y_2' as the variable greatly simplifies the experimental analysis. We may choose the direction of the $\mu_2 = 0$ line ($\vec{\mu}_1$ direction) arbitrarily, and therefore take

$$\mu_2 = T/T_t - 1 \ . \tag{2.6}$$

Now, at fixed T we have from Eqs. (2.4) and (2.2)

$$Y_2' = \frac{\mu_1}{\mu_2^\phi} - \frac{\mu_1^c}{\mu_2^\phi} = \frac{H - H_c(T)}{H_t \mu_2^\phi} \ , \tag{2.7}$$

where $H_c(T)$ is the actual critical field for temperature T. We need not specify μ_1 further except to require it to be of the form

$$\mu_1 = (H/H_t - 1) + f(T - T_t) \ , \tag{2.8}$$

where $f(T - T_t)$ can be any function which vanishes at T_t. Note that $Y_2' = 0$ is the equation of the second-order line.

The two quantities of interest here are the nonordering magnetization and the specific heat. The magnetization relative to the tricritical point is defined as $m = M(T)/M_t - 1$, and has the scaling form [which may be derived from Eq. (2.1)]

$$m(T,H) = \mu_2^{(1-\alpha_t)\phi} m^*(Y_2') \ , \tag{2.9}$$

where $m^*(Y_2')$ is a scaling function which can be derived from an approximate equation of state.[17] A particularly simple form which has the proper behavior is

$$m^*(Y_2') = (\text{const}) \int_{-K}^{Y_2'} |z|^{-\alpha} |z + K|^{(\alpha - \alpha_t)} dz \ . \tag{2.10}$$

For the scaling of the heat capacity, we start from the scaled free energy

$$G(\mu_1, \mu_2) = \mu_2^{(2-\alpha_t)\phi} G^*(\mu_1/\mu_2^\phi) \ . \tag{2.11}$$

The singular part of the heat capacity in constant internal field C_H is given by

$$C_H \sim -\left[\frac{\partial^2 G}{\partial \mu_2^2}\right]_{\mu_1} \sim \mu_2^{(2-\alpha_t-2/\phi)\phi} C^*(Y_2) \ , \tag{2.12}$$

where

$$C^*(Y_2) = \lambda(\lambda - 1) G^*(Y_2) - (2\lambda - \phi - 1)\phi Y_2 G^{*\prime}(Y_2) + \phi^2 Y_2^2 G^{*\prime\prime}(Y_2) \ ,$$

$\lambda = (2 - \alpha_t)\phi$, and prime means differentiation with respect to Y_2. The exponent for the specific heat in constant field is then

$$\bar{\alpha} = \alpha_t - 2 + 2/\phi \ , \tag{2.13}$$

as found previously by Reatto.[18]

The measured heat capacity is taken in constant applied field H_a, so that we must consider C_{H_a}, which is

related to C_H through[19]

$$C_{H_a} = C_H + NT\left(\frac{\partial M}{\partial T}\right)_H^2 \left[1 + N\left(\frac{\partial M}{\partial H}\right)_T\right]^{-1} . \quad (2.14)$$

Using the scaling form for M, we can readily show that

$$\left(\frac{\partial M}{\partial T}\right)_H \sim \frac{\partial^2 G}{\partial \mu_2 \partial \mu_1} = \mu_2^{\phi(1-\alpha_t)-1}[G^{*\prime}(Y_2) - \phi Y_2 G^{*\prime\prime}(Y_2)]$$

and

$$\left(\frac{\partial M}{\partial H}\right)_T \sim \frac{\partial^2 G}{\partial \mu_2^2} = \mu_2^{-\phi\alpha_t} G^{*\prime\prime}(Y_2) .$$

The most singular part of the second term in Eq. (2.14) is

$$T\left(\frac{\partial M}{\partial T}\right)_H^2 \left(\frac{\partial M}{\partial H}\right)_T^{-1} = \mu_2^{\phi(2-\alpha_t-2/\phi)} \times \frac{[G^{*\prime}(Y_2) - \phi Y_2 G^{*\prime\prime}(Y_2)]^2 T}{G^{*\prime\prime}(Y_2)} \quad (2.15)$$

so that the leading singularity of the second term also scales with $\bar{\alpha}$. Therefore, the specific heat at constant applied field has the same scaling form as the internal field heat capacity; that is,

$$C_{H_a}(H,T) = \mu_2^{-\bar{\alpha}\phi} C_{H_a}^*(Y_2') , \quad (2.16)$$

but with a complicated scaling function.

B. Logarithmic corrections

Because the fourth-order term in the Ginzburg-Landau-Wilson free energy vanishes at the tricritical point, classical (Gaussian-model) critical exponents, given in Table I, are predicted.[5] Sixth-order fields are required for stability, and lead to logarithmic corrections to scaling. To discuss these, it is convenient to let the scale factor l in Eq. (2.1) satisfy $l\mu_1^{\phi} = 1$ and take $H_s = 0$. We then obtain

$$G(\mu_1, \mu_2) = \mu_1^{(2-\alpha_t)} g^*(\mu_2/(\mu_1)^{1/\phi}) . \quad (2.17)$$

Wegner and Riedel[6] first obtained the logarithmic corrections to Eq. (2.17) by means of Wilson's approximate recursion relations. They found that μ_2 is corrected in Eq. (2.17) by a factor

$$[l_0 + \ln(\mu_1)]^{1/2-p} \quad (2.18)$$

with $p = 2(n+4)/(3n+22)$. For an Ising ($n=1$) metamagnet, $p = \frac{2}{5}$, so that the logarithmic correction is raised to a small fractional power and is not important except very close to the tricritical point. The constant l_0 is nonuniversal which reflects the fact that the logarithmic corrections are model dependent.

More recently, SAS[7] calculated the logarithmic corrections by diagrammatic methods with quite different results. In their analysis the scaling axis μ_1 is replaced by

$$\mu = \mu_1 - K\mu_2^{\phi} \quad (2.19)$$

so that μ vanishes along the *uncorrected* critical line. The logarithmic correction factor is defined in terms of a field r which vanishes along the logarithmically *corrected* (and presumably experimentally observed) critical line. The correction factor may be written in terms of r as

$$L(r) = 1 - a_6 \ln(r) . \quad (2.20)$$

The constant a_6 is also nonuniversal and is proportional to the amplitude of the sixth-order term in the Hamiltonian. To remain consistent with SAS we also use the notation $Q \equiv \mu_2$.

The Q direction is defined to be everywhere tangent to the mean-field critical line, $\mu = 0$. The relationship between r and μ, given by SAS, is

$$r = \mu + \frac{5}{6}\frac{(n+2)}{(6-n)}\frac{(3n+22)Q^2}{480\pi^2 a_6}[L^{1-2p}(r) - 1] , \quad (2.21)$$

where n is the number of degrees of freedom of the order parameter; $n=1$ here. As we shall see, a_6 is of order unity for $FeCl_2$, so that the difference between r and μ is negligible except very close to the critical line. We choose to use the empirical position of the critical line and use $r \cong \mu \cong [H - H_c(T)]/H_t$ in our analysis.

The expression for the free energy analogous to Eq. (2.17) is[7]

$$G(\mu, Q) = \mu^{(2-\alpha_t)} L^{1-p}(r) g^*(QL^{1/2-p}(r)/\mu^{1/\phi}) . \quad (2.22)$$

A form more suitable to our purposes, similar to Eq. (2.11) is

$$G(\mu, Q) = Q^3 L^{2-3p}(r) G^*(\mu/Q^2 L^{1-2p}(r)) , \quad (2.23)$$

where we have used the classical values $\alpha_t = \frac{1}{2}$ and $\phi = 2$. Note that Eqs. (2.22) and (2.23) are equivalent to Eqs. (2.17) and (2.11), respectively, when $a_6 = 0$. From Eq. (2.23) it is not difficult to derive the scaling forms of the nonordering magnetization and the specific heat. They are

$$m(H,T) = QL^{1-p}(r) m^*(\mu/Q^2 L^{1-2p}(r)) , \quad (2.24)$$

$$C_{H_a}(H,T) = QL^{2-3p}(r) C_{H_a}^*(\mu/Q^2 L^{1-2p}(r)) . \quad (2.25)$$

SAS also make an explicit prediction for the jump

in the magnetization across the first-order line. This expression is somewhat more complicated, but has the form

$$\frac{\Delta m}{|Q|} \propto L^{1-2p}(4r) - \frac{1}{30\pi}\left(\frac{5u_6}{2}\right)^{1/2} L^{1/2-p}(r) \ , \qquad (2.26)$$

where r is now given by

$$r = (5Q^2/8u_6)L^{1/2-p}(r) \ . \qquad (2.27)$$

SAS relate u_6 to a_6, finding $u_6 = \frac{96}{5}\pi^2 a_6$ while Nicoll and Chang[20] give $u_6 = \frac{12}{5}a_6$, a smaller value. The second term in Eq. (2.26) turns out to be negligible in both cases.

The major difference between SAS and WR is the appearance of the logarithmic correction as a factor in the free energy itself—not only in the scaling variable. What is more, the fractional power of this factor is much larger. In Secs. III–V, we will analyze the experimental magnetization and specific heat in three ways: first with classical exponents in the scaling equations (2.9) and (2.16); second, allowing the exponents to vary in these equations; and finally, according to Eqs. (2.24) and (2.25).

III. EXPERIMENT

A. Simultaneous heat-capacity and magneto-optical rotation measurements

The heat-capacity measurement is based on the ac calorimetric method as described by Garnier.[21] The chopping frequency was chosen to be 1.6 Hz, with temperature oscillations of 10 mK rms.

The rotating-polarizer method was used to determine the magneto-optical rotation. This makes use of a rotating plane polarizer to produce a linearly polarized beam, whose polarization direction rotates at the angular velocity Ω of the rotating polaroid. Following an analyzer, a photodetector will detect a sinusoidal signal of frequency 2Ω. An optically active sample between polarizer and analyzer causes an additional rotation in polarization direction, thereby producing a phase shift in the 2Ω signal. That additional phase shift is detected by a phase-detecting analog and digital circuit which communicates with an LSI-11 microcomputer. Data acquisition is under computer control and, with a 16-bit scaler, the resolution is better than 0.01 deg with $\Omega = 50$ Hz. However, mechanical instability of the rotating polaroid limited the resolution to about 0.1 deg.

In order to make the heat-capacity and the magneto-optical rotation measurements compatable, a hot mirror and a He-Ne line spike filter were used. The chopped ir light for the ac heat-capacity measurement is transmitted through the hot mirror, but is stopped by the spike filter. On the other hand, the

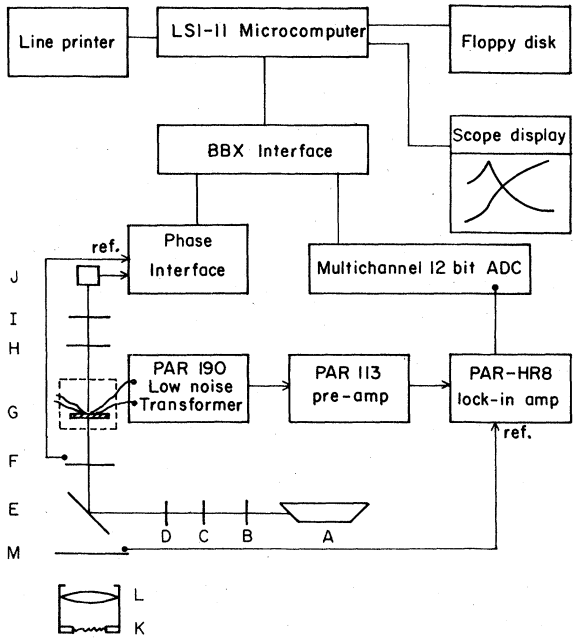

FIG. 2. Experimental setup for simultaneous heat-capacity and optical measurement. *A* He-Ne laser; *B* neutral density filter; *C* polarizer; *D* quarter-wave plate; *E* hot mirror; *F* rotating polarizer; *G* sample; *H* spike filter; *I* analyzer; *J* detector; *K,L* lamp and condenser; *M* chopper.

He-Ne laser beam is reflected by the hot mirror and directed to the sample. The experimental arrangement is sketched in Fig. 2. It is also possible to monitor the intensity of the transmitted light and thereby to locate the mixed phase through the onset of strong light scattering.

B. Sample preparation

Single crystals of ferrous chloride were grown in a conical quartz tube by the Bridgman method. The crystals as grown are 12-mm OD cylinders about 20 mm long with dark brown color. X-ray Laue diffraction shows a D_{3d} point-group symmetry, and chemical microanalysis gives an impurity concentration of less than 0.1% with atomic ratio Fe:Cl = 1:1.98.

As ferrous chloride is very hygroscopic, great care has to be taken during storage and handling. Thin platelike pieces of single crystal were cleaved from the bulk crystal in a glove bag. In order to hold the sample crystalline c axis parallel to the optical axis, the planar sample was sandwiched between two punched pieces of Mylar sheet and mounted in the sample holder. The temperature of the sample holder block is measured by a carbon glass thermometer, which is insensitive to the magnetic field. This carbon glass thermometer was calibrated against a factory-calibrated germanium thermometer in zero

field from 6 to 30 K.

The temperature oscillations of the sample are detected by one of a pair of Chromel-Constantan thermocouples (25 μm diameter) held in thermal contact with the sample by a small amount of Apiezon N grease. The temperature of the sample differs from the sample holder block temperature by a small dc temperature rise which comes from the constant part of the ac power input. This small dc temperature difference, usually on the order of 0.1 deg, is measured by a microvoltmeter through the other portion of the sample thermocouple. A small aperture, 2 mm in diameter, immediately behind the sample, assures that the laser beam passes through the sample in the neighborhood of the thermocouple junction; this ensures that both the heat-capacity and optical-rotation measurements are done at the same position on the sample, at the same temperature, and in the same magnetic field.

Temperature of the sample block is maintained by a temperature controller which uses a capacitance thermometer as sensor and is totally insensitive to magnetic field. The temperature of the outside copper jacket was controlled by separate GaAs diode sensor and heater system. By maintaining the copper jacket only a few degrees below the sample block temperature, we can stabilize the sample environment and achieve good long-term temperature stability of the sample, ~20 mK for each isothermal scan of 30 min.

IV. RESULTS AND INTERPRETATION

As ferrous chloride is extremely hygroscopic and fragile, it proved advisable to use a new sample for each experiment. Each sample, after being mounted, was cooled to liquid-helium temperature and not subsequently cycled to temperatures far above the Néel temperature (23 K). A typical path at 14.1 K is shown in Fig. 3, in which the magnetic field was swept at about 0.04 kOe/sec. The heat capacity, magneto-optical rotation, and the ac amplitude of the optical signal were recorded simultaneously and are displayed as a function of the applied field. The two mixed-phase boundaries show up consistantly in all the three curves although least clearly in the heat capacity. At this temperature the rotation data in the mixed-phase region are not a linear function of field, suggesting that our laser-detector arrangement, which only looks at a very small region of the sample, fails to measure the average magnetization in the mixed-phase region. The strong scattering by the sample when in the mixed-phase region was found to be the most sensitive probe of the mixed-phase boundaries. We divide our investigation into two main regions: $T > T_t$—the second-order region—and $T < T_t$—the first-order region. In the high-temperature region,

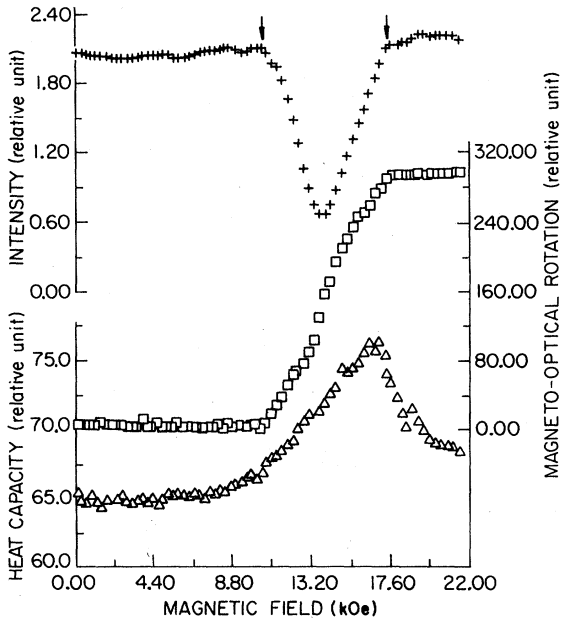

FIG. 3. Typical sweep of applied field at 14.1 K.

we measured heat capacity C_{H_a} and magneto-optical rotation θ_F simultaneously. In the low-temperature region, heat capacity and light scattering were measured simultaneously.

A. Second-order region

The sample used in the high-temperature region had dimensions $4 \times 5 \times 0.10$ mm^3. In order to determine the proportionality constant V between magnetization and rotation, several isothermal scans were taken at temperatures below T_t. In this region, the boundaries of H_a^+ and H_a^- of the mixed phase region

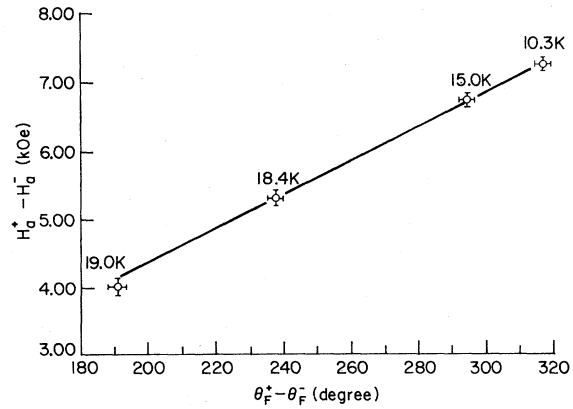

FIG. 4. Applied field differences across the mixed phase vs change in Faraday rotation angle.

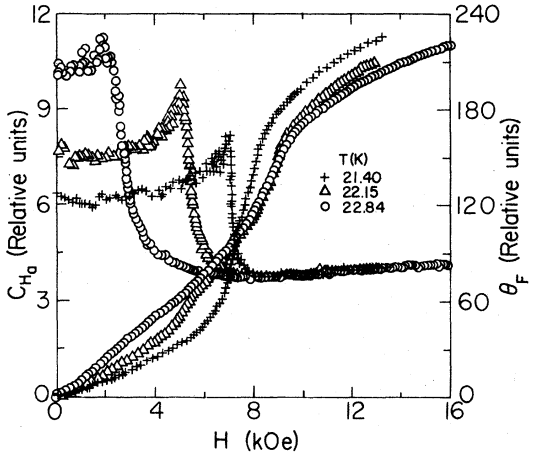

FIG. 5. Specific-heat and Faraday rotation data above the tricritical temperature.

can be easily determined and we have

$$H_a^+ - H_a^- = (N/V)(\theta_F^+ - \theta_F^-) \ , \tag{4.1}$$

since the internal field is constant throughout the mixed phase. The proportionality constant (N/V) is determined from a plot of $(H_a^+ - H_a^-)$ vs $(\theta_F^+ - \theta_F^-)$ for different isotherms below T_t, as in Fig. 4. For this particular sample we determined that $N/V = 0.0228 \pm 0.001$ kOe/deg, independent of temperature.

Ten isotherms were measured for temperatures above T_t, several of which are shown in Fig. 5. Note that the peaks in heat capacity correspond to the inflection points in rotation—these points determine the critical line $H_c(T)$. From double logarithmic plots of $|\theta_F - \theta_F(H_c)|$ vs $|H - H_c|$ (see Fig. 6) for different isotherms and for both $H > H_c$ and

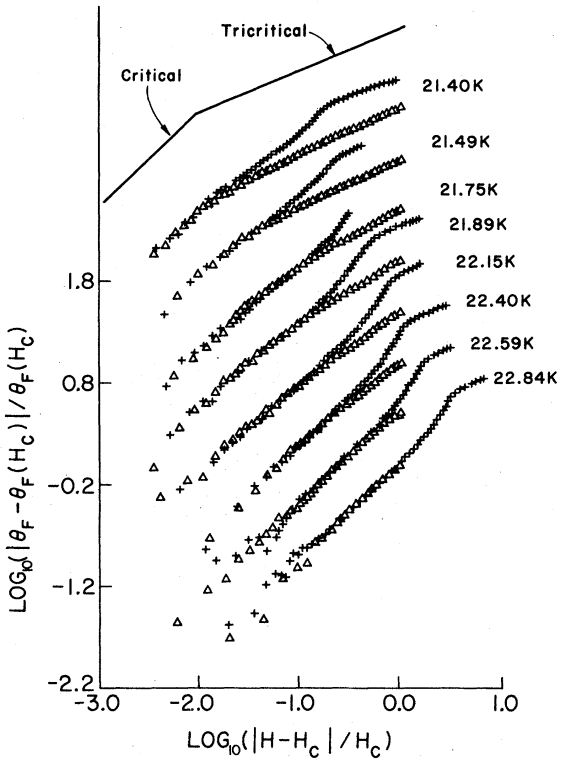

FIG. 6. Rotation data above T_t. Lines have slopes 0.88 (critical) and 0.35 (tricritical) corresponding to $\alpha = 0.12$ and $\alpha_t^{\text{eff}} = 0.65$.

$H < H_c$, we find those data close to the critical line to approach a limiting slope corresponding to $\alpha = \alpha' = 0.12 \pm 0.02$. This asymptotic region is larger the further the isotherm is above T_t. Those data away from the critical line tend to approach another limiting slope corresponding to $\alpha_t^{\text{eff}} = \alpha_t'^{\text{eff}} = 0.65$

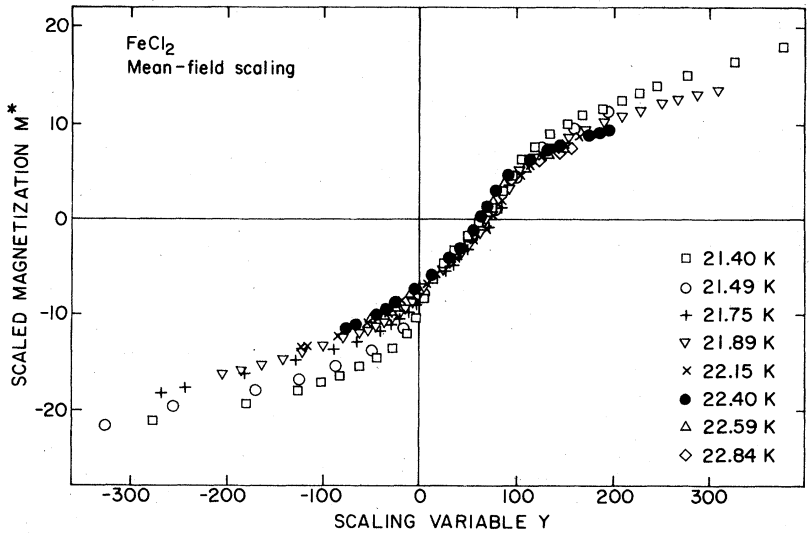

FIG. 7. Scaled magnetization data vs scaling variable using mean-field exponents [cf. Eq. (2.9)].

± 0.05 which is our effective tricritical exponent. This crossover from critical to tricritical behavior is smooth within the antiferromagnetic phase, but it has an additional shoulderlike structure within the paramagnetic phase (see Fig. 6).

Data from eight isotherms between T_t and T_N were used to test the scaling hypothesis (2.9). The magnetization was computed directly from the rotation data as

$$m = [\theta_F(H,T)/\theta_F(H_t,T_t) - 1] \ . \tag{4.2}$$

The fields μ_2 and Y_2' were determined from Eqs. (2.6) and (2.7), respectively. A test of Eq. (2.9) with classical exponents is shown in Fig. 7 for the best choice of H_t, T_t, and $\theta_F(H_t,T_t)$. The failure of the data to fall on a single curve violates the scaling hypothesis. By varying α_t, however, good data collapsing can be obtained with $H_t = 7.7$ kOe, $T_t = 20.54$ K, $\theta_F(H_t,T_t) = 125$ deg, $\alpha_t^{\text{eff}} = 0.65 \pm 0.05$, and $\phi = 2.0$, as shown in Fig. 8.

Finally, we test for the presence of logarithmic corrections as predicted by Eq. (2.24) with results shown in Fig. 9. We take

$$r \cong \mu = [H - H_c(T)]/H_t \ . \tag{4.3}$$

The nonuniversal constant is found to be $a_6 = 0.5 \pm 0.2$ with $T_t = 20.62$ K. The fit is excellent, but not significantly better than the use of a nonclassical value of α_t, as in Fig. 8. This is easy to understand. Examining Eq. (2.22) we find that it can be placed in scaling form by ignoring the factor $L^{1/2-p}(r)$, which deviates only slightly from unity and replacing the factor $\mu^{3/2}L^{1-p}(r)$ by a power of μ. Over the experimentally accessible range, we find

$$\mu^{3/2}L^{1-p}(r) \sim \mu^{1.35} \equiv \mu^{2-\alpha_t^{\text{eff}}} \ . \tag{4.4}$$

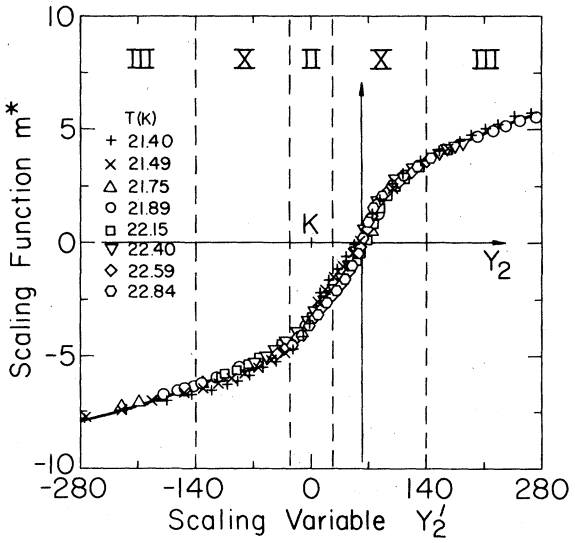

FIG. 8. Data of Fig. 7 scaled with the effective critical exponent $\alpha_t^{\text{eff}} = 0.65$. The solid line is the prediction of the model scaling function, Eq. (2.10).

Thus, the fact that the logarithmic correction mimics a power law over a restricted range of data makes it difficult to detect unambiguously. The effective scaling exponent simulates scaling in all respects. For example, we have fitted the approximate scaling function (2.10) to the data of Fig. 8 by adjusting only K and the proportionality constant and using $\alpha_t^{\text{eff}} = 0.65$ and $\alpha = 0.12$ with the result shown as a solid line in Fig. 8. As may be seen, this function reproduces even the asymmetry of the scaling function around the critical line.

According to Eq. (2.16) it should be possible to scale the specific heat in a manner similar to the

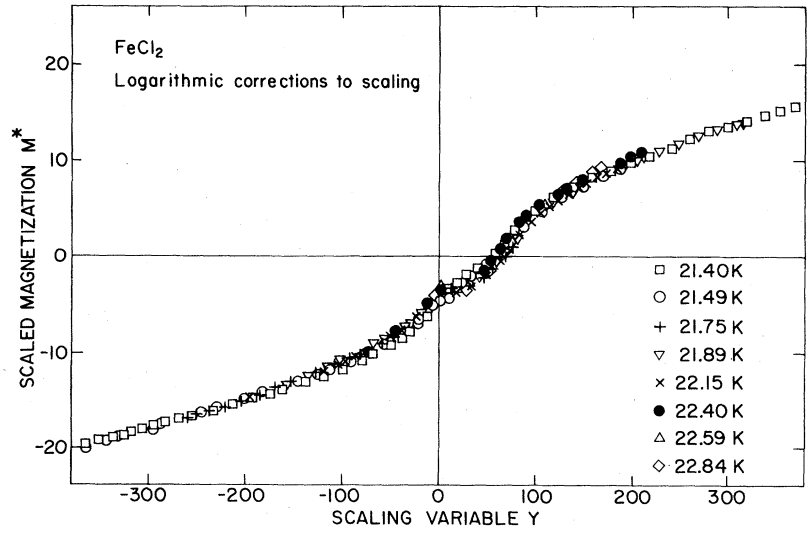

FIG. 9. Data of Fig. 7 scaled according to Eq. (2.24) with classical exponents and logarithmic corrections.

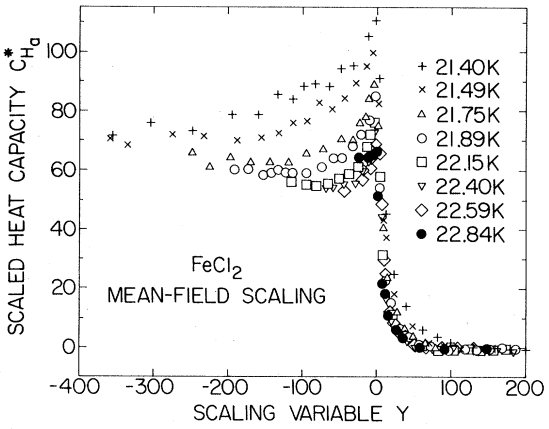

FIG. 10. Heat-capacity data for $T > T_t$ scaled with classical exponents according to Eq. (2.16).

magnetization. The specific-heat data, however, contain a lattice background term which cannot be expected to scale. Consequently, we have subtracted a common background from all the data, which causes them to approach zero at high values of the scaling variable. This results in complete collapsing of all the data to zero far above the critical line. However, below and near the critical line, the specific heat provides a sensitive test of scaling. This may be seen in Fig. 10 where the heat-capacity data have been scaled with the classical value of the exponent $\bar{\alpha} = -\frac{1}{2}$, as obtained from Eq. (2.13) with $\phi = 2$ and $\alpha_t = \frac{1}{2}$. Very large deviations from scaling behavior are apparent. A dramatic improvement occurs with the effective exponent $\alpha_t^{\text{eff}} = 0.65$, for which $\bar{\alpha} = -0.35$, as seen in Fig. 11. Inclusion of the logarithmic correction factor according to Eq. (2.25), with a_6 fixed at the value obtained from the previous analysis of the magnetization ($a_6 = 0.5$), along with $\bar{\alpha} = -\frac{1}{2}$ also

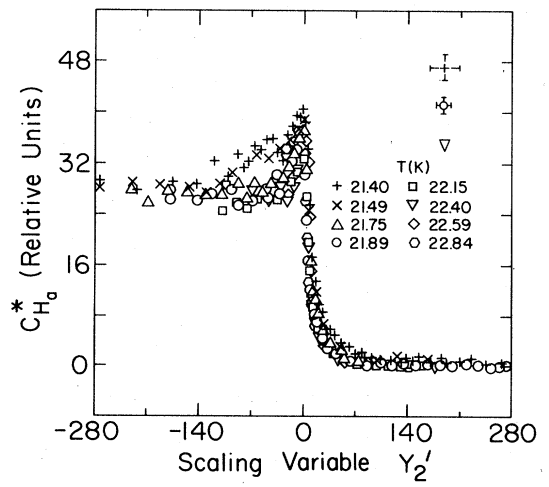

FIG. 11. Heat-capacity data from Fig. 10 scaled with the effective exponent $\bar{\alpha} = -0.35$.

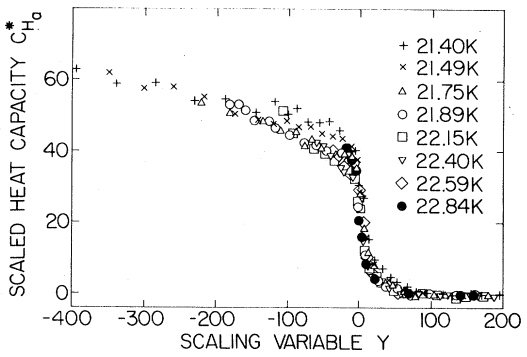

FIG. 12. Heat-capacity data scaled according to Eq. (2.25) with classical exponents and the same logarithmic corrections used in Fig. 9.

greatly improves the scaling fit as shown in Fig. 12.

A remarkable feature of the logarithmically corrected scaling of the heat-capacity data is the disappearance of the peak in the scaling function at the critical line. This is related, we believe, to the fact that the specific heat at constant applied field is a constrained quantity whose singular behavior is renormalized.[18] This means that the correction term (2.15) tends to cancel the singularity in C_H^*.

The ability to scale both the heat capacity and the nonordering magnetization with classical exponents and the same logarithmic correction factors lends strong support to our assertion that logarithmic corrections are important. We have tabulated the effective exponents for $FeCl_2$ in Table I, along with values for other metamagnets. It appears that the same corrections will be important, with similar coefficients for $CsCoCl_3 \cdot 2H_2O$.

B. First-order region

The mixed-phase region has been studied by means of light scattering, for which a thicker sample of dimensions $4 \times 5 \times 0.16$ mm^3 was used. The transmitted intensity and the heat capacity of this sample for a typical isotherm (19.14 K) are shown in Fig. 13. The mixed-phase boundaries are clearly delineated by the region of strong light scattering. Less obvious, but noticeable, are the jumps in heat capacity at the limits of the mixed phase. These are the result of the latent heat of the first-order transition and have been discussed extensively elsewhere.[15]

The phase boundaries in the vicinity of the tricritical point have been determined for this sample and are shown in Fig. 14. The points below the tricritical temperature were determined from the onset and disappearance of light scattering, while those above T_t are located from the peak in the heat capacity. The data agree exactly with those obtained on the thinner sample and reported above. The jump in nonordering magnetization can be determined direct-

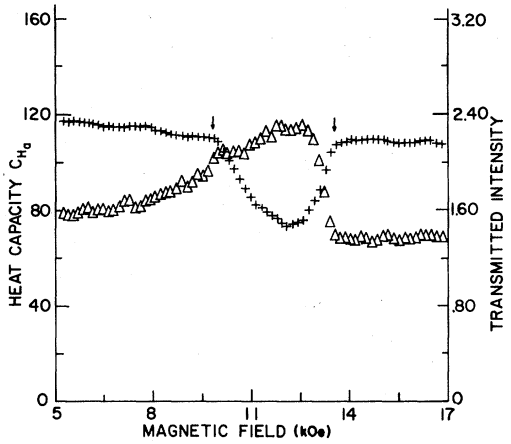

FIG. 13. Typical data in the mixed-phase region at 19.14 K.

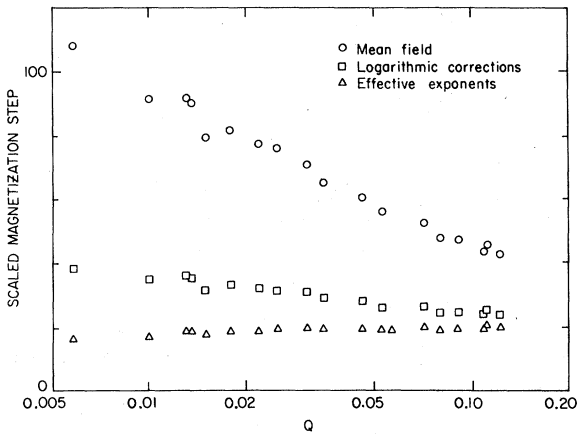

FIG. 15. Scaling of the magnetization jump across the first-order line. Circles are for $\Delta m/|Q|$; triangles, for $\Delta m/|Q|^{0.63}$—the effective exponent; and squares, for $\Delta m/|Q|L^{0.6}(4r)$ as predicted by Eq. (2.26).

ly from the scattering data since

$$\Delta m = N(H_a^+ - H_a^-) \ , \tag{4.5}$$

due to the constancy of the internal field in the mixed phase. According to the usual scaling theory, Δm should vanish with $|Q|$, corresponding to a critical exponent $\beta_\mu = 1$. In order to test this prediction, we have plotted $\Delta m/|Q|$ vs $|Q|$ in Fig. 15. Clearly, there is a strong Q dependence remaining, rather than the constant predicted by scaling theory. Logarithmic corrections have been calculated by SAS and were given in Eq. (2.26). However, the relationship between our parameter a_6 and the coefficient u_6 is not certain. Using the SAS result that $u_6 = \frac{96}{5}\pi^2 a_6$ we find that the logarithmic corrections do not explain the deviations from mean-field behavior seen in Fig. 15. However, the Nicoll and Chang result that $u_6 = \frac{12}{5} a_6$ greatly improves the situation. In both cases we have solved Eq. (2.27) numerically for r at each value of Q. The result is shown in Fig. 15, where the squares are plots of $\Delta m/|Q|L^{0.6}(4r)$. Some Q dependence remains. A better fit can be obtained with effective exponents, as seen from the constancy of $\Delta m/|Q|^{0.63}$, triangles in Fig. 15. The effective exponent $\beta_u = 0.63$ is consistent with $\beta_u^{\text{eff}} = (1 - \alpha_t^{\text{eff}})\phi$ when the exponent $\alpha_t^{\text{eff}} = 0.65$, determined above, is used (cf. Table I).

The results along the first-order line, therefore, are better fitted with effective exponents than with logarithmic correction factors. There is, however, considerable latitude in the logarithmic factors. The definition of r along the critical line is determined by u_6 which is in turn related to a_6 through the logarithmic correction factor. With some adjustment of the constants, especially a decrease in u_6 relative to a_6, better agreement could be obtained.

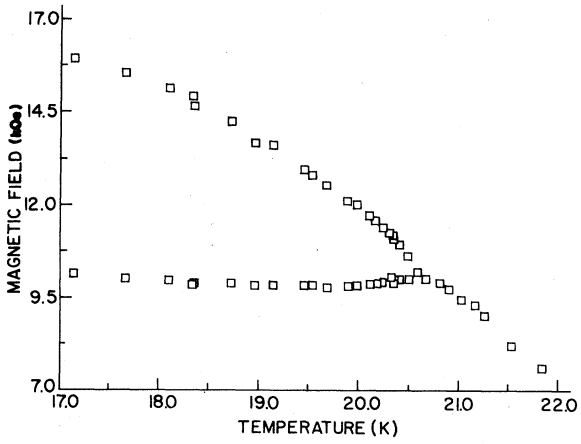

FIG. 14. Phase diagram in the vicinity of the tricritical point. Data below T_t is from light scattering; above, from heat-capacity peaks.

V. DISCUSSION

Although the nature of the tricritical point in three dimensions is, it is said, a solved problem, there are serious discrepancies between theory and experiment for metamagnets. In Table I, we have listed the experimental results available for several metamagnets, along with the mean-field predictions. While some exponents agree with theory, most do not. A comparison of our *effective* exponents with those obtained by Bongaarts and de Jonge[13] shows a remarkable degree of agreement. These values, although uncertain, cannot be made to agree with theory simply by adjusting the location of the tricritical point nor the definitions of the scaling fields.

We have shown in this paper that the deviations of the exponents from their classical values are the

result of logarithmic correction factors which are predicted to be present. Recent calculations by SAS,[7] by Nicoll and Chang,[20] and by Yamazaki and Suzuki[22] have shown these corrections to be stronger than originally predicted.[6] The difference is the presence of a correction to the free energy itself, with a larger power of the correction factor than for the scaling fields. We have treated the coefficient which appears in the correction factor as an adjustable parameter, and have shown that once chosen, it suffices to correct both the nonordering magnetization and the specific heat in a way which recovers the classical exponents. Along the first-order line, the correction improves the agreement with classical exponents, but does not completely remove the discrepancies.

Large deviations such as occur for metamagnetic tricritical behavior do not appear to occur in ^{3}He-^{4}He mixtures.[8] This indicates that the nonuniversal coefficient a_6, which we have found to be on the order of 0.5, must be considerably smaller for ^{3}He-^{4}He mixtures. Our results seem to be strong evidence for the nonuniversality of logarithmic corrections—an issue clearly in need of further investigation.

ACKNOWLEDGMENTS

We gratefully acknowledge the support of the NSF through Grant No. 78-07763 and the helpful comments of Professor M. Wortis.

---

*Present address: Bell Telephone Laboratories, Crawford Hill Laboratory, Holmdel, N.J. 07733.

[1]L. Landau, Phys. Z. Sowjetunion 11, 26 (1937).
[2]R. B. Griffiths, Phys. Rev. Lett. 24, 715 (1970).
[3]E. K. Riedel, Phys. Rev. Lett. 28, 675 (1972).
[4]T. S. Chang, A. Hankey, and H. E. Stanley, Phys. Rev. B 8, 346 (1973).
[5]E. K. Riedel and F. J. Wegner, Phys. Rev. Lett. 29, 349 (1972).
[6]F. J. Wegner and E. K. Riedel, Phys. Rev. B 7, 2481 (1973).
[7]M. J. Stephen, E. Abrahams, and J. P. Straley, Phys. Rev. B 12, 256 (1975).
[8]E. K. Riedel, H. Meyer, and R. P. Behringer, J. Low Temp. Phys. 22, 369 (1976).
[9]E. Stryjewski and N. Giordano, Adv. Phys. 26, 487 (1977).
[10]N. Giordano and W. P. Wolf, Phys. Rev. Lett. 35, 799 (1975); N. Giordano and W. P. Wolf, in *Magnetism and Magnetic Materials-1975 (Philadelphia)*, edited by J. J. Becker, G. H. Lander, and J. J. Rhyne, AIP Conf. Proc. No. 29 (AIP, New York, 1976), p. 459.
[11]J. A. Griffin and S. E. Schnatterly, Phys. Rev. Lett. 33, 1576 (1979); J. F. Dillon, E. Yi Chen, and H. J. Guggenheim, Phys. Rev. B 18, 377 (1978).
[12]R. J. Birgeneau, G. Shirane, M. Blume, and W. C. Koehler, Phys. Rev. Lett. 33, 1098 (1974).
[13]A. L. M. Bongaarts and W. J. M. de Jonge, Physica (Utrecht) 86-88B, 595 (1977).
[14]M. J. Stephen, J. Phys. C 13, L83 (1980).
[15]H-T. Shang, C-C. Huang, and M. B. Salamon, J. Appl. Phys. 49, 1366 (1978); H-T. Shang and M. B. Salamon, in *Proceedings at the International Conference on Magnetism*, edited by W. Zinn, G. Kalvius, and E. Feldtkeller (North-Holland, Amsterdam, 1980), p. 419; H-T. Shang and M. B. Salamon, Phys. Rev. Lett. 44, 879 (1980).
[16]R. B. Griffiths, Phys. Rev. B 7, 545 (1973).
[17]D. R. Nelson and J. Rudnick, Phys. Rev. Lett. 35, 178 (1975).
[18]L. Reatto, Phys. Rev. B 5, 204 (1972).
[19]P. M. Levy and D. P. Landau, J. Appl. Phys. 39, 1128 (1968); D. P. Landau, B. E. Keen, B. Schneider, and W. P. Wolf, Phys. Rev. B 3, 2310 (1971).
[20]J. F. Nicoll and T. S. Chang, Phys. Lett. A 64, 477 (1978).
[21]P. R. Garnier, Ph.D. thesis (University of Illinois, 1972) (unpublished).
[22]Y. Yamazaki and M. Suzuki, Prog. Theor. Phys. 58, 1369 (1977).